Please cite the Published Version

Assessment of Hydraulic Network Models in Predicting Reverse Flows in OD Cooled Disc Type Transformer Windings

XIANG ZHANG [ID], (Member, IEEE), AND ZHONGDONG WANG [ID], (Senior Member, IEEE)

School of Electrical and Electronic Engineering, The University of Manchester, Manchester M13 9PL, U.K.

Corresponding author: Zhongdong Wang (zhongdong.wang@manchester.ac.uk)

ABSTRACT Predicting liquid flow distribution in the winding is crucial for transformer thermal design and hydraulic network models are usually used to guarantee reasonable liquid flow distribution. This paper is a continuation of the research effort in using computational fluid dynamics (CFD) to calibrate and improve the network modelling approach. The possibility is assessed of hydraulic network models in predicting the occurrence of reverse flows in pump-driven oil directed (OD) cooling modes. CFD modelling shows that the occurrence of reverse flows requires both high Reynolds number at the winding pass inlet and the ''real'' pass inlet velocity profile. To reflect the effect of pass inlet velocity profile on flow distribution, a winding pass is added beneath dividing and merging junctions in deriving minor pressure loss correlations. In addition, hybrid minor loss correlations are used to incorporate the effect of pass inlet velocity profile and to mitigate the inaccuracy of minor pressure loss segregation introduced by the inclusion of a winding pass beneath the junctions. Even with the above mentioned improvements, a conventional network model with one node for each junction still cannot predict reverse flows because of its architecture limit, hence a 3-node junction network model is then proposed. It is demonstrated that the newly developed 3-node junction hydraulic network model can predict the occurrence of reverse flows in OD cooled disc-type transformer windings.

INDEX TERMS Hydraulic network model, hybrid correlation, junction 3-node, reverse flow, transformer.

I. INTRODUCTION

Liquid-immersed power transformers with disc-type windings are the most common transformer type in the transmission power network, where the liquid servers as a dielectric as well as a coolant. The liquid flow distribution in the winding pass has a direct impact on the cooling performance and affects the highest temperature in the winding, which determines the highest thermal ageing rate of the cellulose insulation and therefore the normal life expectancy of the transformer [1], [2].

For pump-driven oil directed (OD) cooling modes, the effect of buoyancy force is negligible [3], leaving the hydraulic design being the focus. Ideally, the liquid flow distribution should match the power loss distribution in the winding. However, in reality, an even flow distribution is desired to avoid localized overheating arising from uneven flow distribution.

The hydraulic design of the transformer may be based on empirical formulae and evolutions of manufacturer experience. However, it becomes more challenging as new design features can well emerge outside the empirical comfort zone. Modelling of the hydraulic system is therefore increasingly recognized as a trend.

Two modelling methods are available: hydraulic network and computational fluid dynamics (CFD). The two methods share the same principles of mass and momentum conservation, with network models being composed of nodes and branches reduced from original flow topology and using correlations to describe pressure drops in relation to geometry and flow conditions [4]–[9] and, on the other hand, CFD models solving the governing differential equations in a direct numerical manner [10], [11]. CFD models provide more reliable and detailed results over network models at the expense of much more complicated model setting-up process and much higher computational requirement.

Off-the-shelf correlations for the so called ''minor pressure losses'' from fluid mechanics literature are found inaccurate

The associate editor coordinating the review of this manuscript and approving it for publication was Tao Wang [ID].

and lead to significant discrepancies in flow and pressure drop results between network models using these correlations and CFD models. CFD calibration of the correlations following the literature correlation format is implemented in [12] and the resulted pressure drop prediction over the winding is greatly improved [13]. Pronounced improvements of the "minor loss" correlations from CFD are achieved by multi-layer curve fitting of the "minor pressure loss" coefficients with their controlling parameters derived from dimensional analysis [14]. A typical hydraulic network model equipped with the "minor loss" correlations from [14] proves to be capable of generating flow distribution and winding total pressure drop results that are comparable with CFD results.

CFD simulations and experimental tests show that for OD cooling modes with the increase of the Reynolds number (Re) at the winding pass inlet the liquid flow distribution becomes increasingly uneven with higher flow rates in the top horizontal ducts and lower flow rates in the bottom horizontal ducts. In addition, reverse flows can occur at high Re's [3], [8], [15], and it is detrimental to the insulation as the reverse flow region has a low net flow rate that causes localized overheating. To avoid reverse flows in a transformer the hydraulic design tool needs to be capable of predicting its occurrence in the first place. For a network model to predict the occurrence of reverse flows, it needs to be equipped with minor loss correlations corresponding to reverse flow scenarios, and it should switch to the right correlations when the flow pattern changes and reverse flows occur.

This paper is a continuation of the effort in improving network modelling by CFD calibration. It assesses hydraulic network models in predicting reverse flows in OD cooled disc-type transformer windings and proves that a hydraulic network model, if set in a proper format, can predict this phenomenon. Section II presents the development of a conversional hydraulic network model and compares flow distribution and winding total pressure drop results from the developed model with those obtained from the network model in [14] and a CFD model. The developed model and its modified versions are then applied to predicting the occurrence of reverse flows in section III, followed by conclusion in section IV.

II. DEVELOPMENT OF HYDRAULIC NETWORK MODEL
A. HYDRAULIC NETWORK MODEL FRAMEWORK
In a conventional hydraulic network model [4]–[9], the winding hydraulic topology is reduced to a network of nodes at junctions and branches connecting the nodes. Mass conservation is applied to each node or the sum of pressure drop in a closed loop is equalized to 0. The flow rate in a branch is determined by the pressure drop over the branch and the hydraulic resistance of the branch.

There are two types of hydraulic resistance, one relating to the so-called major pressure loss due to friction and the other relating to the so-called minor pressure losses due to changes of flow direction.

The hydraulic resistance in a planar 2D duct due to friction (R_f) for a hydraulically fully developed flow is

$$R_f = \frac{96 \cdot \mu \cdot l}{D_h^3} \qquad (1)$$

where μ stands for dynamic viscosity, l for duct length, D_h for duct hydraulic diameter (twice the duct height). The friction resistance for fully developed flow is only related to the geometry and the dynamic viscosity of the liquid.

The minor hydraulic resistance, on the other hand, is related to the geometry, the liquid properties (density and viscosity) and the mass flow split. In disc-type windings, there are five types of flow configurations relating to the so-called minor pressure losses, as shown in Fig. 1. Taking the dividing scenario as an example, the dividing pressure drops in the radial (Δp_{dr}) and axial (Δp_{da}) directions are related to the corresponding pressure loss coefficients and the dynamic pressure at the axial inlet,

$$\Delta p_{dr} = K_{dr} \cdot \frac{1}{2} \rho v_1^2 \qquad (2)$$

$$\Delta p_{da} = K_{da} \cdot \frac{1}{2} \rho v_1^2 \qquad (3)$$

where K_{dr} and K_{da} stand for dividing pressure loss coefficient in radial and axial direction respectively, ρ for density and v_1 for average inlet velocity.
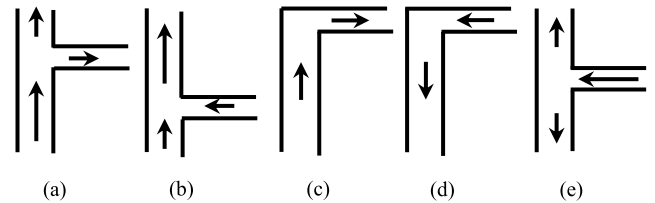
FIGURE 1. Flow configurations relating to "minor" pressure losses. (a) dividing, (b) merging, (c) elbow with inlet at axial duct, (d) elbow with inlet at radial duct, (e) reverse dividing.

The dividing radial resistance (R_{dr}) and dividing axial resistance (R_{da}) as shown in Fig. 2 (b) are in the following format

$$R_{dr} = \frac{2 \cdot K_{dr} \cdot \dot{m}_2}{D_h^2 \cdot \beta^2} = \frac{2 \cdot K_{dr} \cdot \dot{m}_{inlet}^2}{D_h^2 \cdot \dot{m}_2} \qquad (4)$$

$$R_{da} = \frac{2 \cdot K_{da} \cdot \dot{m}_3}{D_h^2 \cdot (1-\beta)^2} = \frac{2 \cdot K_{dr} \cdot \dot{m}_{inlet}^2}{D_h^2 \cdot \dot{m}_3} \qquad (5)$$

where $\dot{m}_{inlet}$, $\dot{m}_2$ and $\dot{m}_3$ is the mass flow rate in the inlet, the radial and axial dividing ducts, respectively, β is the mass flow fraction in the radial duct, as denoted in Fig. 2 (a).

The pressure loss coefficients (e.g. K_{dr} and K_{da}) are controlled by the geometry ($\alpha = H_r/H_a$, the ratio of radial duct height to axial duct width), the flow split (β) and the Reynolds number (Re) at the inlet [14]. It is worth noting that the effect of rounding radius of the winding discs on pressure loss and flow distribution in the winding is found negligible and therefore it is not included in the analysis.
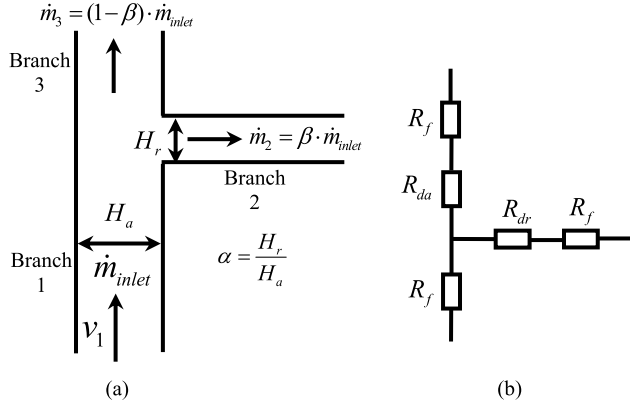
FIGURE 2. Hydraulic resistances in a flow dividing scenario. (a) Dividing flow configuration, (b) Network representation of the flow dividing scenario.

The minor hydraulic resistances are related to the flow rates in the branches, indicating that iterations must be conducted to solve a hydraulic network model. A typical hydraulic network model for a 4-radial-duct winding pass is shown in Fig. 3.
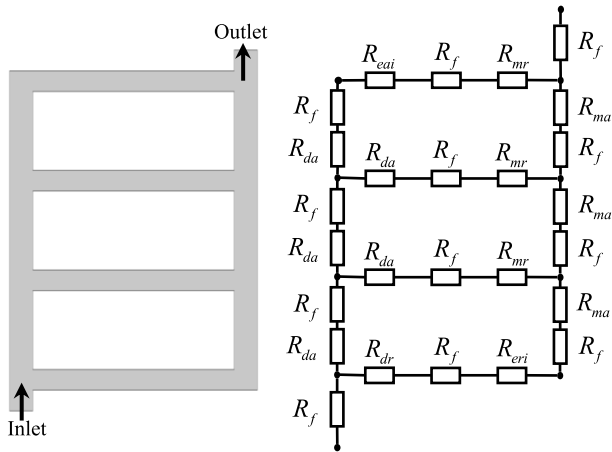
FIGURE 3. A typical hydraulic network of a 4-radial-duct winding pass. R_f for friction resistance, R_{dr} for dividing radial resistance, R_{da} for dividing axial resistance, R_{mr} for merging radial resistance, R_{ma} for merging axial resistance, R_{eai} for elbow resistance with axial inlet flow, R_{eri} for elbow resistance with radial inlet flow.

B. MINOR LOSS COEFFICIENT CORRELATIONS

Dimensional analyses show that the minor loss coefficients for dividing, merging and flows over elbows are controlled by Re at the inlet, geometry (α), and flow split (β for flows over elbows is 1) [14]. To quantify the minor loss coefficients, isothermal CFD simulations of the flow configurations, shown in Fig. 1, are performed. In the CFD simulations, the inlet velocity profile is set fully developed and the other branches are long enough so that the flows after passing the junction can regain fully developed conditions. With fully developed conditions maintained at the outlets the minor losses over the junction can be segregated from the friction

losses. The drawback of this arrangement is that the interactions between ducts in affecting minor losses are dismissed. Detailed simulation strategies follow closely that presented in [12], [14]. It is worth mentioning that a pass-by-pass consideration of the liquid flow distribution accounting for the duct flow interaction was proposed in [15] to correlate flow fraction with pass inlet Re directly.

CFD parametric sweeps of Re, α and β for the 5 minor loss related configurations are summarized in Table 2. Re is defined at the branch with the total flow rate and α is the ratio of radial duct height to axial duct width. In conventional scenarios, β refers to the ratio of radial duct flow rate to the total flow rate. In reverse dividing scenarios, which are not included in conventional hydraulic network models, β refers to the mass flow ratio of the lower axial duct to that of the radial duct and this ratio is limited to 0.5 because of the symmetry of the flow configuration. The pressure loss coefficient for lower axial duct with $\beta > 0.5$ is identical to that of upper axial duct with lower axial duct mass flow ratio being $1 - \beta$.

Multilayer least-square curve fitting strategy is adopted to form a correlation between the pressure loss coefficient and its controlling parameters. The fitting functional format set for a generic pressure loss coefficient is shown in (6).

$$
\begin{cases}
K = \dfrac{a_1}{\mathrm{Re}} + a_2 \cdot \ln(\mathrm{Re}) + a_3 \\
a_i = b_{i1}\alpha^3 + b_{i2}\alpha^2 + b_{i3}\alpha + b_{i4} \ (i \in \{1,\ 2,\ 3\}) \\
b_{ij} = c_{ij1}\beta^3 + c_{ij2}\beta^2 + c_{ij3}\beta + c_{ij4} \ (j \in (\{1,\ 2,\ 3,\ 4\})
\end{cases}
\tag{6}
$$

where a and b coefficients are dummy coefficients and 48 c-coefficients are generated. For elbow pressure loss coefficients the third layer is not included and 12 b-coefficients are generated.

Since the minor loss coefficients for (a)-(d) in Fig. 1 are almost identical to those shown in [14], only the results for reverse dividing with α being 0.3 are shown in Fig. 4 and Fig. 5 as representative results. It is worth noting that reverse dividing junctions are not included in traditional network model. However, it is needed to model reverse flow scenarios. The data points shown in black circle are CFD results and the meshes are generated by correlation equation sets. The maximum errors between the CFD results and those from the correlations are 0.029 for pressure loss coefficient in the lower axial duct and 0.028 for the upper axial duct, and these errors are negligible in affecting flow predicting.
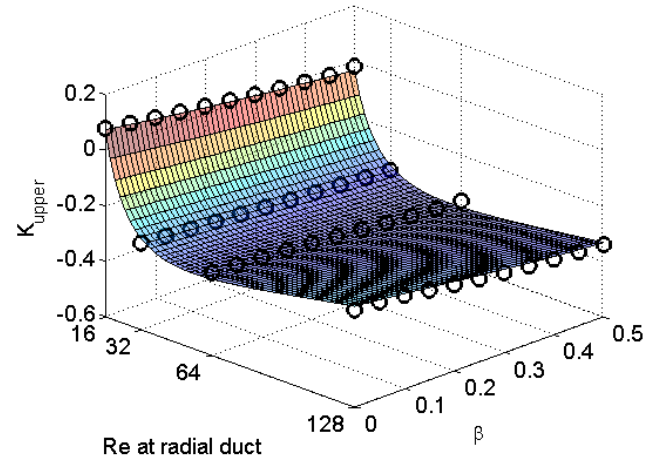
C. IMPLEMENTATION OF HYDRAULIC NETWORK MODEL

For a conventional 1-pass network model, when the number of horizontal ducts is n, there will be $2n+2$ nodes and $3n$ branches. The topmost node is usually set as a reference node with the pressure assigned to be 0. Each branch has a flow rate and the hydraulic resistance of the branch is contributed by both "major" and "minor" pressure losses. The formats of "major" and "minor" resistances are shown by (1), (4) or (5) respectively.
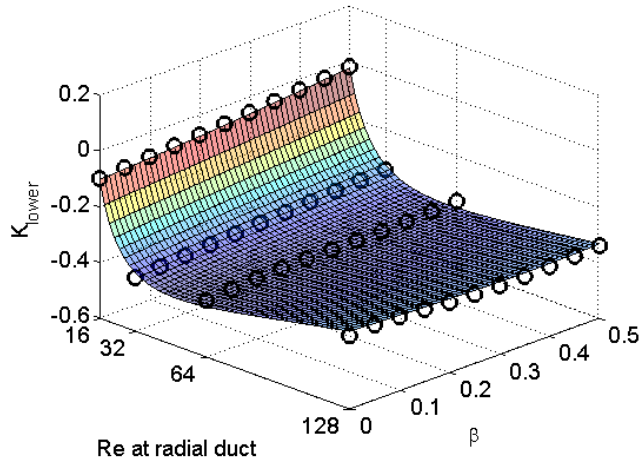
FIGURE 4. Pressure loss coefficients in the lower axial duct for reverse dividing T-junctions. Black circles are data points from CFD and the mesh is generated by the correlation equation set.

TABLE 1. Parametric sweep ranges for minor loss related configurations.

	Dividing	Merging	Axial inlet elbow	Radial inlet elbow	Reverse dividing
Re	64, 128, 256, 512, 1024, 1400	64, 128, 256, 512, 1024, 1400	32, 64, 128, 256, 512	32, 64, 128, 256, 512	16, 32, 64, 128
α	0.2, 0.3, 0.4, 0.5, 0.6, 0.7	0.2, 0.3, 0.4, 0.5, 0.6, 0.7	0.2, 0.3, 0.4, 0.5, 0.6, 0.7	0.2, 0.3, 0.4, 0.5, 0.6, 0.7	0.2, 0.3, 0.4, 0.5, 0.6, 0.7
β	0, 0.01, 0.03, 0.05, 0.1, 0.2, 0.3, 0.4, 0.5, 0.6, 0.7	0, 0.01, 0.03, 0.05, 0.1, 0.2, 0.3, 0.4, 0.5, 0.6, 0.7	1	1	0, 0.01, 0.03, 0.05, 0.1, 0.2, 0.3, 0.4, 0.5, 0.6, 0.7

Nodal analysis is adopted for the 2n+1 nodes. If we assume the hydraulic conductance (reciprocal of hydraulic resistance) between nodes *i* and *j* is Y_{ij}, we can write the nodal equations as
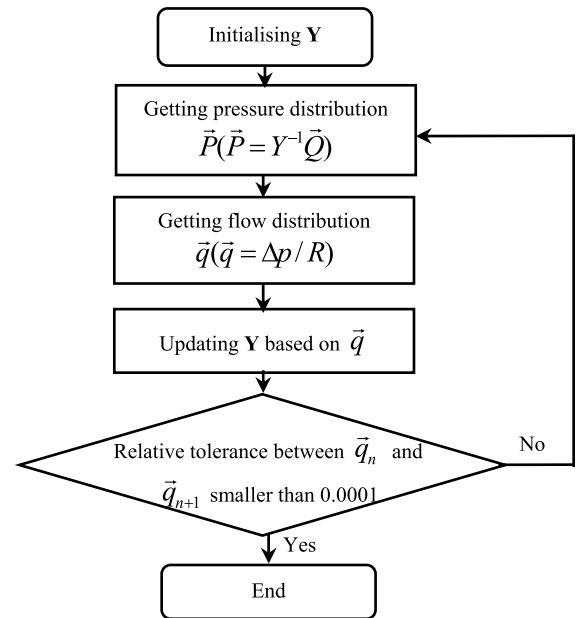
$$\mathbf{Y} \cdot \vec{P} = \vec{Q}$$

where **Y** is a (2n+1)×(2n+1) hydraulic conductance matrix; $\vec{P}$ and $\vec{Q}$ are (2n+1) ×1 pressure vector and flow source vector respectively. It is worth noting that the $\vec{Q}$ elements are all zeros except for the bottom node, which has a flow source of the pass inlet flow rate.

Since the "minor" hydraulic resistance is flow rate and flow distribution dependent as described in section *II A*, the hydraulic conductance matrix needs to be updated iteratively when a new flow distribution is obtained until the change of the hydraulic conductance matrix (**Y**) is negligible. The flow chart of implementing the network model is shown in Fig. 6.
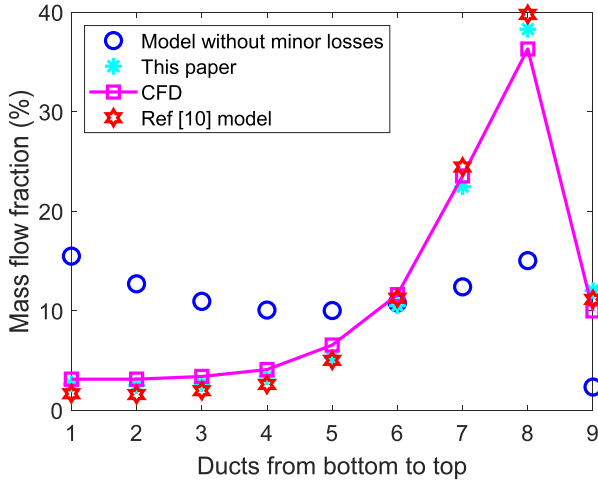
D. COMPARISONS
The hydraulic network model developed is compared with that in [14] and a CFD model for an isothermal OD flow

FIGURE 5. Pressure loss coefficients in the upper axial duct for reverse dividing T-junctions.


FIGURE 6. Flow chart for hydraulic model implementation.

over a 1-pass disc-type winding. The winding has 8 discs of the dimension of 88 × 12 mm, two axial ducts both being 6 mm wide, 9 radial ducts with radial ducts 1-8 at the bottom being 4 mm high and the top radial duct being 2 mm high. The Reynolds number at the pass inlet is 1001. The results for mass flow distribution in the winding and static pressure drop over the winding are compared and shown in Fig. 7 and TABLE 2, respectively. The network models developed in this paper and that in [14] give comparable flow distribution and pressure drop results to those obtained from the CFD model. The so-called minor pressure losses have significant influence on the flow distribution and the total pressure drop. This is shown by a network model that ignores the minor pressure losses and gives totally different flow distribution and pressure drop results.

FIGURE 7. Comparisons of mass flow distributions from 3 network models and a CFD model.

TABLE 2. Comparisons of pressure drops over the winding model.

	Network model without minor losses	Network model of this paper	Ref. 10 network model	CFD
Δp (Pa)	131.33	278.79	263.56	275.35
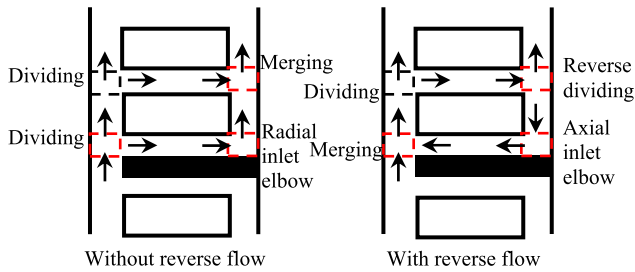
FIGURE 8. Changes of junction types when a reverse flow occurring at the bottom of the pass. The red boxes denote the changes of junction type.

III. PREDICTING REVERSE FLOWS

For OD cooling modes when Re at the winding pass inlet is high enough, reverse flows occur in the bottom radial ducts of winding passes, which are observed in both CFD simulations [8], [15], [16] and experimental measurements [3], [17].

For a hydraulic network model, reverse flows occur in one of the two conditions: (1) the static pressure drop over the radial duct is reversed and the total hydraulic resistance in the radial duct is positive; (2) the static pressure drop over the radial duct is not reversed and the total hydraulic resistance is negative. When a reverse flow occurs, some junction types change accordingly, e.g. when a reverse flow occur at the pass bottom radial duct, the junction type changes are shown in Fig. 8.

In this section we explore the possibility of predicting flow reversal by 3 types of modified hydraulic network models: a conventional 1-node junction network model with reverse

dividing minor loss correlations, 1-node junction network model with hybrid minor loss correlations, and a new 3-node junction hydraulic network model and hybrid minor loss correlations. The following 3 sub-sections present the performance of the three types of models in predicting the occurrence of reverse flow.

A. CONVENTIONAL 1-NODE JUNCTION NETWORK MODEL
Liquid flow distributions for a 2-pass winding model, as shown in Fig. 9 (a), are investigated by planar 2D CFD simulations. The reason to choose this winding model is that the CFD flow distribution results have been verified by experimental tests using particle image velocimetry techniques [3].
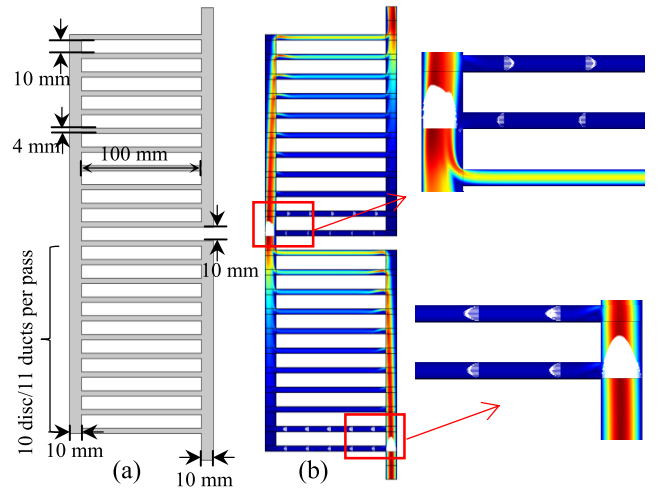

FIGURE 9. 2-pass winding model. (a) Geometry (b) Velocity contour at Re=1200.

CFD shows that pass 1 and pass 2 have different flow patterns. When pass inlet Re is 1200, pass 2 experiences reverse flow at the bottom horizontal duct but no reverse flows in pass 1, as shown by the velocity profiles in Fig. 9 (b). In fact, even when pass inlet Re increases to 2000, pass 1 experiences no reverse flows. In addition, CFD shows that for the flow reversed radial duct at the bottom of pass 2, the pressure drop is reversed, i.e. the average pressure at the expected duct inlet is lower than that at the expected outlet, indicating the total hydraulic resistance in the flow reversed radial duct is still positive. Therefore, the first condition specified at the beginning of this section is the reality.

The occurrence of reverse flows requires not only high Re but also the pass inlet velocity profile from the upstream pass outlet, which is a velocity profile with its peak shifted away from the middle of the duct to the wall side, as shown by the upper-right close-up in Fig. 9 (b). For pass 1 or a 1-pass CFD winding model, the pass inlet velocity profile is usually prescribed to be uniform or parabolic and herein lies the reason why pass 1 or a 1-pass CFD model cannot have reverse flows.

Network models share the same physical principles with CFD but with lower spatial resolution, and the way minor loss
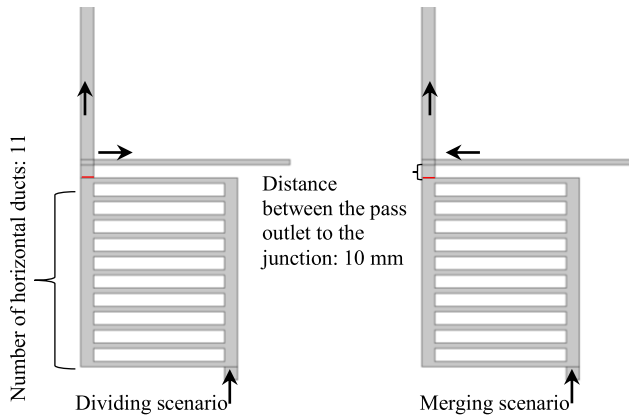
FIGURE 10. Dividing and merging junctions with the modified inlet condition of a winding pass located beneath. In CFD simulations, the axial branch is longer than that shown in the figure to guarantee fully developed condition at the outlet.

TABLE 3. Hybrid minor loss correlations.

	Dividing	Merging	Axial inlet elbow	Radial inlet elbow	Reverse dividing
Conventional junctions	Other than pass inlet	Axial minor losses	All	All	All
Junctions with a pass beneath	Pass inlet radial and axial minor losses	Radial minor losses	None	None	None

correlations are extracted, as shown in [12], [14], cannot take into account the effect of winding pass inlet velocity profiles. Therefore, a conventional hydraulic network model even with reverse dividing minor loss correlations cannot describe or predict the occurrence of reverse flow.

B. 1-NODE JUNCTION NETWORK MODEL WITH HYBRID CORRELATIONS

To make a hydraulic network model capable of predicting the occurrence of reverse flow, the effect of winding pass inlet velocity profile has to be taken into account in establishing the pressure loss correlations. Therefore, a winding pass is added to the bottom of the dividing and merging junction axial inlets, as shown in Fig. 10. It is worth noting that the number of horizontal ducts in the winding pass beneath and the distance between the pass outlet to the junction affect the minor pressure losses. However, results from a typical condition of 11 horizontal ducts and pass outlet to junction distance being 10 mm are representative. Planar 2D CFD parametric sweeps of Re, α and β in the ranges shown in TABLE 1 for dividing and merging junctions with a pass of the typical conditions attached beneath are implemented to take into account the effect of junction inlet velocity profile.

The drawback of having the upstream pass outlet velocity profile is that the pressure at the junction inlet (the pass outlet), shown as red lines in Fig. 10, is not uniform, and average pressures have to be taken when deriving the minor pressure losses. Because of this approximation the minor pressure losses cannot be segregated exactly from the friction pressure losses. To mitigate this uncertainty, hybrid minor pressure loss correlations derived from junction CFD simulations with and without a winding pass beneath are used in the network model developed, as shown in **TABLE 3**. For the winding pass inlet, it is essential to use dividing radial and axial pressure loss correlations derived from junctions with a pass beneath. In addition, the merging radial pressure loss correlations derived from junctions with a pass beneath can

be used as well because it is not directly related to the junction axial inlet.

The comparisons of flow distributions in pass 1 and pass 2 for pass inlet Re being 1200 from CFD and network models with conventional and hybrid minor loss correlations are shown in Fig. 11. The ducts in a pass are named from bottom to top. Flow distributions in pass 1 from CFD and conventional network model show no reverse flows with the maximum flow deviation of 3.32% at the penultimate duct between the two models. Flow distributions in pass 2 from CFD and the network model with hybrid correlations show similar trend with maximum deviation being 1.3% at the bottom of the winding pass. CFD shows the reverse flow at the bottom duct (-1.3%), and the network model with hybrid correlations shows the lowest flow rate at the bottom duct (1.5×10^{-9} %) very close to 0 but not reversed. Since the flow is not reversed, the changes of junction type shown in Fig. 8 are not triggered in the network model developed. The so close to 0 flow rate in the bottom radial duct is caused by the inverse proportional relationship between the minor loss resistance and the flow rate in the branch as shown by (4) and (5). The lower the radial duct flow rate, the higher the radial dividing resistance and this higher resistance feeds back into an even lower radial duct flow rate and so on. It is worth emphasizing that the hydraulic network model with the hybrid minor loss correlations compares well with CFD results, though the occurrence of reverse flow cannot be captured.

C. 3-NODE JUNCTION HYDRAULIC NETWORK MODEL WITH HYBRID CORRELATIONS

To enable a hydraulic network model to predict the occurrence of reverse flow, extra nodes at the junction need to be added to allow detailed liquid flow split at the junction and pressure drop reversal over radial ducts without violating the principle of the sum of the pressure drops in a closed loop being 0. Instead of using 1 node at the center of the junction, 3 nodes are prescribed for 3 types of junctions: dividing, merging and reverse dividing, as shown in Fig. 12. No extra nodes are needed for the two types of elbow junctions because flows in elbows are not split.

With 3 nodes prescribed, 6 minor loss hydraulic resistances are generated. 5 scenarios, each with 6 minor loss correlations, are involved, including dividing with and without a pass beneath the junction, merging with and without a pass
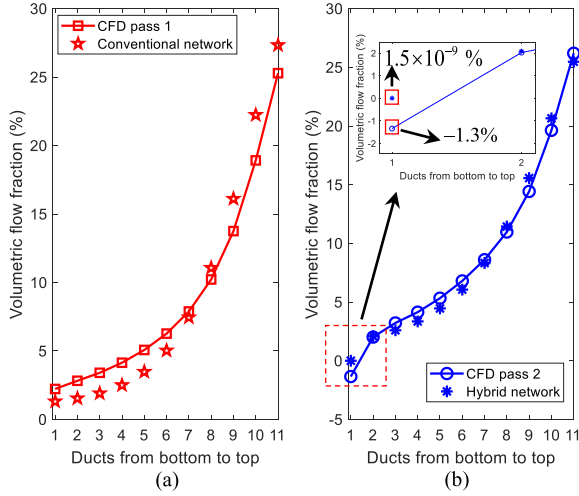
FIGURE 11. Flow distribution comparisons with pass inlet Re being 1200. (a) Pass 1 flow distributions from CFD and a network model with conventional minor pressure loss correlations; (b) Pass 2 flow distributions from CFD and a network model with hybrid minor pressure loss correlations.
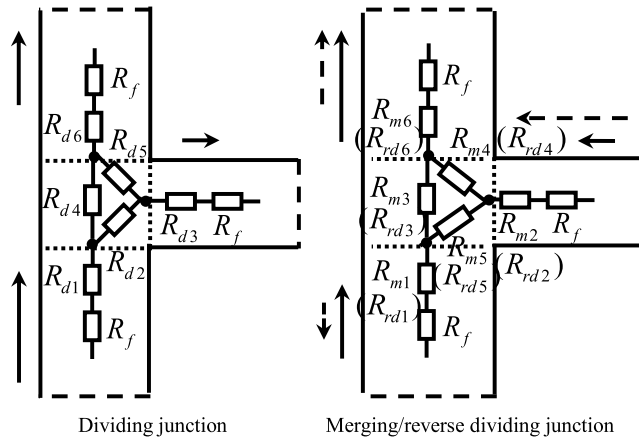

FIGURE 12. Three-node dividing, merging and reverse dividing junctions. Subscript f stands for friction, d for dividing m for merging and rd for reverse dividing.

beneath the junction, and reverse dividing without a pass attached to the junction. For each junction type or scenario, CFD parametric sweeps of Re, α and β shown in TABLE 1 are used and correlations for the corresponding 6 minor loss coefficients are formed.

Similar to the 1-node junction network model with hybrid correlations, the 3-node junction network model adopts hybrid correlations as well. The hybrid correlations are shown in TABLE 4. All the 6 minor loss correlations for the pass inlet dividing junction are from the CFD parametric sweeps of junctions with a pass beneath to modify its inlet condition, while the other dividing junction correlations are from CFD sweeps without inlet condition modifications. For the merging junctions, minor loss 2, 4 and 6 correlations, which are related to the radial flow path as shown in Fig. 12, are from sweeps with modified inlet

TABLE 4. Hybrid minor loss correlations.

|	Dividing	Merging	Axial inlet elbow	Radial inlet elbow	Reverse dividing
Conventional junctions	Other than pass inlet	Minor loss 1, 3, 5	All 2 minor losses	All 2 minor losses	All 6 minor losses
Junctions with a pass beneath	Pass inlet 6 minor losses	Minor loss 2, 4, 6	None	None	None
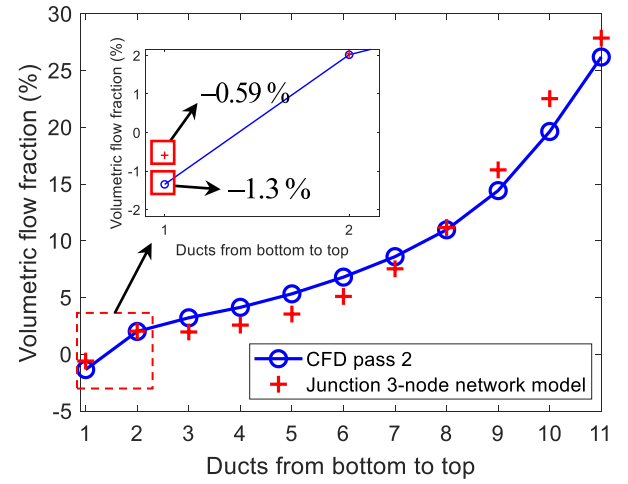
FIGURE 13. Flow distribution comparisons with pass inlet Re being 1200.

conditions and minor loss 1, 3, 5 correlations are from sweeps with fully developed inlet conditions (with no pass attached beneath).

With 3 nodes for the dividing, merging and reverse dividing junctions, a winding pass with n radial ducts ends up with $6n-2$ nodes and $9n-6$ branches. The network is solved with the same procedures shown in Fig. 6. The comparison of flow distributions for pass 2 in the 2-pass winding model with Re being 1200 from CFD and the 3-node junction network model is shown in Fig. 13. The 3-node junction network model predicts the occurrence of reverse flow at the bottom radial duct (-0.59%), which triggers the changes of junction type in the bottom of the pass.

The maximum flow fraction deviation between the CFD and the 3-node junction network model is 2.89% at the penultimate duct. Compared to the 1-node junction network model in section III B, the 3-node junction network model results in slightly higher maximum flow discrepancy with the CFD results because the 6 minor losses cannot be exactly segregated from friction losses.

The pressure distribution and flow pattern in the bottom of the pass from the 3-node junction network model are shown in Fig. 14. The reverse flow in the bottom radial duct is caused by pressure drop reversal across the radial duct. In addition, flows across some branches can gain pressure due to negative minor pressure loss coefficients associated with the flow splitting or merging. The flow fractions in the branches in Fig. 14 are shown in TABLE 5. The higher than 100% flow
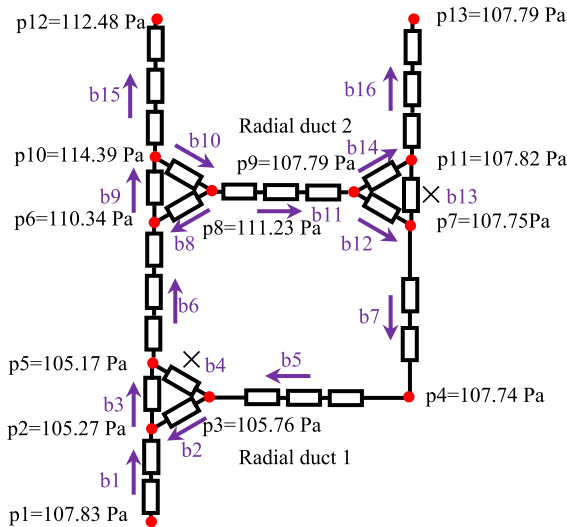
FIGURE 14. Node pressure distribution and flow pattern in the bottom two radial ducts. p stands for pressure, b for branch, and × indicates no flow passing the branch.

TABLE 5. Flow distribution in the bottom 2 radial ducts.

Branch	b1	b2	b3	b4	b5	b6
Flow fraction (%)	100.00	-0.59	100.59	0	-0.59	100.59
Branch	b7	b8	b9	b10	b11	b12
Flow fraction (%)	-0.59	-4.00	104.59	-6.04	2.04	-0.59
Branch	b13	b14	b15	b16		
Flow fraction (%)	0	1.45	98.55	1.45		

Flow from small index node to large index node is designated as positive and vice versa.
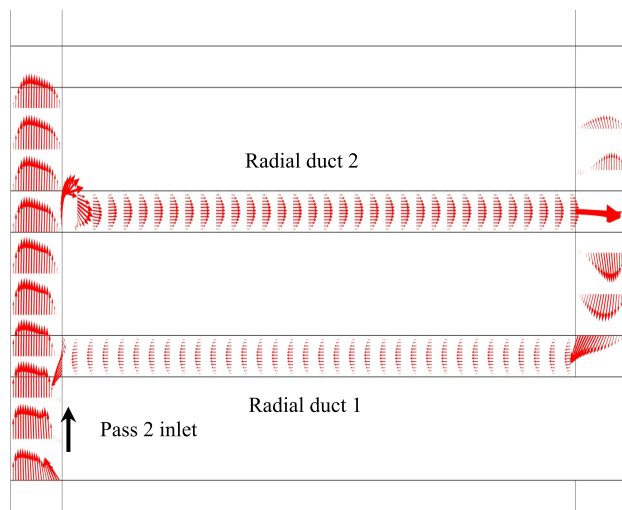
FIGURE 15. Velocity profiles at the bottom of pass 2 from the CFD model. The inlet axial duct scale factor is 0.008, radial ducts scale factor 0.035, outlet axial duct scale factor 0.1.

rates in branch 3 and branch 6 are due to the occurrence of reverse flows in branch 2, 5, 7 and 12.

The network model flow pattern in Fig. 14 is like the flow pattern shown by the CFD velocity profiles in Fig. 15,

for example, the recirculation flow pattern at the entrance of duct 2, reverse dividing at the exit of duct 2 and the reverse merging at the entrance of duct 1. These similar flow distribution and flow pattern prove that the 3-node junction network model can mimic the flow pattern revealed by CFD. It is worth noting that different scale factors are used in Fig. 15 to show velocity profiles of different parts of the winding together.

IV. CONCLUSION

CFD and hydraulic network models are usually used in transformer thermal design to control the liquid flow distribution in the winding. Hydraulic network models with proper minor pressure loss correlations can produce comparable flow distribution results to those from CFD models.

Reverse flows cause localized overheating and are detrimental to insulation. To avoid the occurrence of reverse flow, the thermal design tool should be capable of predicting its occurrence. Studies here show the occurrence of reverse flow requires high Re at the winding pass inlet and the inlet velocity profile from the outlet of the upstream pass. Conventional 1-node junction hydraulic network models do not have reverse dividing junctions and cannot consider the effect of the pass inlet velocity profile and therefore cannot predict reverse flows.

To equip a hydraulic network model the ability to predict reverse flows, correlations for reverse dividing junctions are added and a winding pass is positioned beneath dividing and merging junctions to consider the effect of inlet velocity profiles. To mitigate the inaccuracy in determining the minor losses introduced by the inclusion of a winding pass beneath a junction, hybrid correlations from conventional junctions and junctions with a pass beneath are adopted. However, reverse flows still cannot be predicted due to the limit of the architecture of conventional 1-node junction network model, though the flow rate at the bottom radial duct is predicted to be very close to 0.

The architecture of conventional hydraulic network model is updated with junctions (apart from elbows) represented by 3 nodes to allow representation of pressure drop reversal across radial ducts. The introduction of 3 nodes in the junction brings 6 minor loss related resistances as compared to 2 minor loss related resistances for conventional 1-node junction network. By adopting a similar hybrid correlation strategy, the newly proposed 3-node junction hydraulic network model predicts the occurrence of reverse flow in the winding pass.
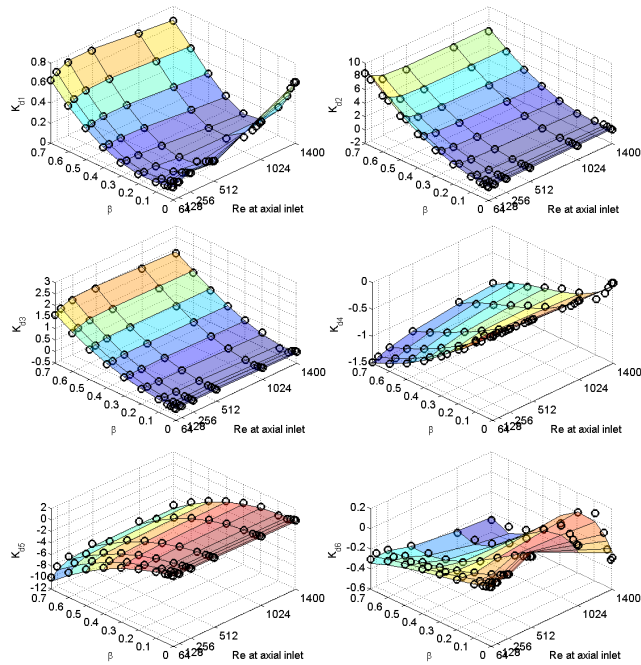
APPENDIX

A 3-node junction generates 6 minor loss related hydraulic resistances. The variation of the 6 minor loss coefficients for a dividing junction with the condition of a pass beneath and α being 0.3 are presented in Fig. 16.

FIGURE 16. Dividing minor loss coefficient K_{d1}, K_{d2}, K_{d3}, K_{d4}, K_{d5}, K_{d6} variations with Re and α is fixed to be 0.3. The black circles are data points from CFD parametric sweeps and the mesh is generated by correlation equation sets.

him to research the feasibility of using network models to predict reverse flows. The authors would also like to express their gratitude to their colleagues Dr Qiang Liu and Prof. Paul Jarman for various internal technical discussions.

REFERENCES

[1] *Loading Guide for Oil-Immersed Power Transformers*, Standard 60076-7, 2018.

[2] *Guide for Loading Mineral-Oil-Immersed Transformers and Step-Voltage Regulators*, IEEE Standard C57.91, 2011.

[3] X. Zhang, M. Daghrah, Z. Wang, Q. Liu, P. Jarman, and M. Negro, "Experimental verification of dimensional analysis results on flow distribution and pressure drop for disc-type windings in OD cooling modes," *IEEE Trans. Power Del.*, vol. 33, no. 4, pp. 1647–1656, Aug. 2018.

[4] A. J. Oliver, "Estimation of transformer winding temperatures and coolant flows using a general network method," *IEE Proc. C Gener. Transmiss. Distrib.*, vol. 127, no. 6, pp. 395–405, Nov. 1980.

[5] J. Zhang and X. Li, "Coolant flow distribution and pressure loss in ONAN transformer windings Part I: Theory and model development," *IEEE Trans. Power Del.*, vol. 19, no. 1, pp. 186–193, Jan. 2004.

[6] Z. R. Radakovic and M. S. Sorgic, "Basics of detailed thermal-hydraulic model for thermal design of oil power transformers," *IEEE Trans. Power Del.*, vol. 25, no. 2, pp. 790–802, Apr. 2010.

[7] E. Rahimpour, M. Barati, and M. Schäfer, "An investigation of parameters affecting the temperature rise in windings with zigzag cooling flow path," *Appl. Therm. Eng.*, vol. 27, nos. 11–12, pp. 1923–1930, 2007.

[8] H. M. R. Campelo, M. A. Quintela, F. Torriano, P. Labbé, and P. Picher, "Numerical thermofluid analysis of a power transformer disc-type winding," in *Proc. IEEE Elect. Insul. Conf. (EIC)*, Montreal, QC, Canada, Jun. 2016, pp. 362–365.

[9] H. M. R. Campelo, L. Braña, and X. M. Lopez-Fernandez, "Thermal hydraulic network modelling performance in real core type transformers," in *Proc. Int. Conf. Elect. Mach. (ICEM)*, Sep. 2014, pp. 2275–2281.

[10] A. Santisteban, F. Delgado, A. Ortiz, I. Fernández, C. J. Renedo, and F. Ortiz, "Numerical analysis of the hot-spot temperature of a power transformer with alternative dielectric liquids," *IEEE Trans. Dielectr. Electr. Insul.*, vol. 24, no. 5, pp. 3226–3235, Oct. 2017.

[11] X. Zhang, Z. Wang, Q. Liu, P. Jarman, and M. Negro, "Numerical investigation of oil flow and temperature distributions for ON transformer windings," *Appl. Therm. Eng.*, vol. 130, pp. 1–9, Feb. 2018.

[12] W. Wu, Z. D. Wang, A. Revell, H. Iacovides, and P. Jarman, "Computational fluid dynamics calibration for network modelling of transformer cooling oil flows—Part I heat transfer in oil ducts," *IET Electr. Power Appl.*, vol. 6, no. 1, pp. 19–27, 2012.

[13] A. Weinläder, W. Wu, S. Tenbohlen, and Z. Wang, "Prediction of the oil flow distribution in oil-immersed transformer windings by network modelling and computational fluid dynamics," *IET Electr. Power Appl.*, vol. 6, no. 2, pp. 82–90, 2012.

[14] J. Coddé, W. Van der Veken, and M. Baelmans, "Assessment of a hydraulic network model for zig-zag cooled power transformer windings," *Appl. Therm. Eng.*, vol. 80, pp. 220–228, Apr. 2015.

[15] X. Zhang, Z. Wang, and Q. Liu, "Prediction of pressure drop and flow distribution in disc-type transformer windings in an OD cooling mode," *IEEE Trans. Power Del.*, vol. 32, no. 4, pp. 1655–1664, Aug. 2017.

[16] A. Weinläder and S. Tenbohlen, "Thermal-hydraulic investigation of transformer windings by CFD-modelling and measurements," in *Proc. 16th Int. Symp. High Voltage Eng.*, Cape Town, South Africa, 2009.

[17] M. Nakadate, K. Toda, K. Sato, D. Biswas, C. Nakagawa, and T. Yanari, "Gas cooling performance in disc winding of large-capacity gas-insulated transformer," *IEEE Trans. Power Del.*, vol. 11, no. 2, pp. 903–908, Apr. 1996.

XIANG ZHANG received the B.Eng. degree in electrical and electronic engineering from Xi'an Jiaotong University, China, in 2012, and the Ph.D. degree in electrical engineering from The University of Manchester, U.K., in 2017, where he is currently a Research Associate with the School of Electrical and Electronic Engineering. His research interest includes transformer thermal modeling. He is a member of CIGRE A2.60 working group on dynamic thermal behavior of power transformers.

ZHONGDONG WANG received the B.Sc. and M.Sc. degrees in high voltage engineering from Tsinghua University, in 1991 and 1993, respectively, and the Ph.D. degree in electrical engineering from UMIST, in 1999. She is currently a Professor of high voltage engineering with the School of Electrical and Electronic Engineering, The University of Manchester. Her research interests include power transformers covering all aspects of modeling and simulation, materials and systems, and asset management policies.

● ● ●